Available online at www.sciencedirect.com

ScienceDirect

Energy Procedia 1 (2009) 3015–3022

Energy Procedia

www.elsevier.com/locate/procedia

GHGT-9

Risk Mitigation Through the Optimization of Residual Gas and Solubility Trapping for CO_2 Storage in Saline Aquifers

Long Nghiem*, Chaodong Yang, Vijay Shrivastava,
Bruce Kohse, Mohamed Hassam and Colin Card

Computer Modelling Group Ltd., 150, 3553 – 31 Street NW, Calgary, Alberta, Canada T2L 2A6

Abstract

The two most important trapping mechanisms in CO_2 storage in saline aquifers, namely residual gas trapping and solubility trapping are examined. It is shown that a water injector located above the CO_2 injector can be used to enhance both residual gas trapping and solubility trapping. Using simulation, the optimal location and operating conditions for the water injector are determined for both a low-permeability aquifer and a high-permeability aquifer. It is shown that low vertical permeability and water injection at a larger depth favor residual gas trapping while high vertical permeability and water injection at a smaller depth favor solubility trapping. It is also shown that for high-permeability aquifers, water injection does not increase the total CO_2 trapping.

Keywords: CO_2 Storage; Saline Aquifers; Residual Gas Trapping; Solubility Trapping; Optimization.

1. Introduction

Saline aquifers represent the most important venue for CO_2 storage since they have the largest capacity of among all other venues (coal seams, depleted gas and oil fields). There are several CO_2 trapping mechanisms in saline aquifers: (1) structural trapping; (2) residual gas trapping; (3) solubility trapping and (4) mineral trapping. Structural trapping involves the storage of CO_2 in a geological structure as a free gas or super-critical fluid. CO_2 can flow and escape through the cap rock or sealing faults if the integrity of the latter is compromised. Residual gas trapping (Kumar et. al., 2005) consists of storing CO_2 as an immobile gas in the porous media. This process has been identified as one of the most important processes for safe CO_2 storage as the immobile gas can be kept away from the cap rock. CO_2 is highly soluble in brine and solubility trapping is essentially the impetus for CO_2 storage in saline aquifers. As CO_2 dissolves in brine, it decomposes into H^+ and HCO_3^-. These ions in turn react with the minerals in place. Depending on the mineralogy of the formation, the reactions could induce precipitation of

* Corresponding author. Tel.: +1-403-531-1319; fax: +1-403-282-6495.
E-mail address: long.nghiem@cmgl.ca

doi:10.1016/j.egypro.2009.02.079

carbonate minerals such as Calcite, Dolomite and Siderite, which represent essentially the conversion of CO_2 into minerals. (Nghiem et al., 2004; Thibeau et al., 2007)

An important goal in CO_2 storage in saline aquifers is to minimize the risk of leakage through the cap rock over the long storage period. The risk of structural trapping is the highest as the CO_2 is mobile and will migrate through the cap rock if there are micro fractures or if the rock fails because of geomechanical and/or geochemical effects. Solubility trapping is safe as CO_2 is stored as a soluble component in brine and will only come out of solution if there is a substantial drop in pressure. This is very unlikely for large aquifers. Nevertheless, there is the potential migration of CO_2 saturated brine over large distances if the aquifer is active. Residual gas trapping is also a safe trapping mechanism, especially if the immobile CO_2 is kept away from the cap rock. Residual gas trapping is induced when CO_2 is injected near the bottom of the aquifer and the CO_2 bubble rises to the top of the aquifer due to gravity segregation. Residual gas trapping has been recognized as the most rapid method to trap CO_2 with time scales in the order of years to decades (Ennis-King and Paterson, 2002; Kumar et. al., 2005; Obi and Blunt, 2006; Juanes et al., 2007; Qi et al., 2007). The conversion of CO_2 into carbonate minerals (Calcite, Dolomite, Siderite), also referred to as mineral trapping, relies on the dissolution of other minerals in the aquifer that provide Ca^{++}, Mg^{++} and Fe^{++} for the conversion (Thibeau et al., 2007). CO_2 mineralization is probably the safest mode for CO_2 storage. However, mineralization takes hundreds or thousands of years and there are many uncertainties in the prediction of the process. From a practical point of view, solubility and residual gas trapping are the two low-risk modes for CO_2 storage that could be designed and predicted with a degree of certainty.

This paper investigates the residual gas trapping mechanism in detail and its application in a low-permeability and high-permeability aquifer. The solubility trapping mechanism is also evaluated in conjunction with residual gas trapping. To simplify the analysis of residual gas trapping and solubility trapping, aquifers with homogeneous permeability and porosity are used. Methods for accelerating and increasing residual gas trapping through water injection are discussed. An optimization procedure is then used to determine the operating conditions that would maximize the combined amount of CO_2 trapped as residual gas and as a soluble component in brine for a low-permeability and high-permeability aquifer. The simulation software used in the study is the geomechemical Equation-of-State compositional simulator GEM™ (Nghiem et. al., 2004). The optimization and sensitivity analysis is carried out with the software CMOST™ (Yang et al., 2007a, 2007b).

2. Residual gas trapping

Residual Gas Trapping is caused by wettability and capillary effects in porous media. The treatment of trapping in this paper follows the hysteresis model of Land (1968). Figure 1 shows the relative permeability curves for CO_2 injection. During injection, when the CO_2 phase (gas phase) saturation increases, the gas relative permeability curve for CO_2 follows the drainage relative permeability curve k_{rg}^{d} (black curve). If at a saturation S_{gi}^{*}, the gas saturation decreases, the relative permeability curve for CO_2 would follow the imbibition curve k_{rg}^{i} (red curve). If the gas saturation continues to decrease until k_{rg} is zero, the residual trapped gas saturation S_{gt}^{*} is reached. In Figure 1, $S_{g,max}$ is the maximum gas saturation and $S_{gt,max}$ is the maximum trapped gas saturation. The Land coefficient is given by

$$C = \frac{1}{S_{gt,max}} - \frac{1}{S_{g,max}} \tag{1}$$

and the residual trapped gas saturation is

$$S_{gt}^{*} \left(S_{gi}^{*}\right) = \frac{S_{gi}^{*}}{1 + C S_{gi}^{*}} \tag{2}$$

where S_{gi}^{*} is the saturation corresponding to flow reversal. Spiteri et al. (2005) provide a summary of other residual gas trapping models.

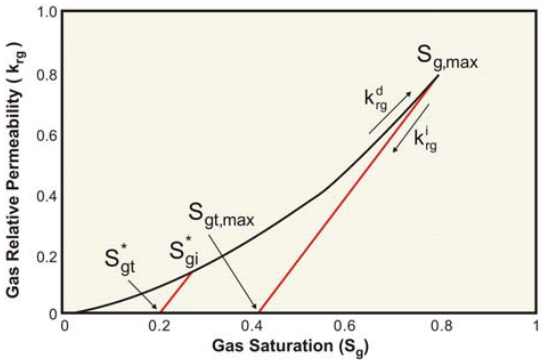

Figure 1 – Land's residual gas trapping model

The following example illustrates the residual gas trapping mechanism that occurs during a CO_2 storage process (Run 1). A quarter of an element of symmetry containing a CO_2 injector is shown in Figure 2. The water injector is shut-in in this case. The porosity is 0.2, the horizontal permeability is 100 md and the vertical permeability is 10 md. The average initial conditions are: pressure = 21,472 kPa; temperature = 79.5ºC and salinity = 32,000 ppm. The grid system is 71 × 71 × 100 = 504,100 with a uniform gridblock size of 15 m × 15 m × 3 m. The aquifer thickness is 300 m and the lateral extent of the element of symmetry is 1065 m. Large volume modifiers (10^7) are applied to the outer boundary gridblocks to represent a constant pressure boundary. CO_2 is injected at a depth of 2276 m (near the bottom of the aquifer) on 2000-01-01 at a rate of 10^6 std m^3/day (1869 ton/day) for a period of 25 years. The cumulative CO_2 injected is 9.1313×10^9 std m^3/day or 1.7068×10^7 tons. Figure 3 shows the gas and water relative permeability curves used in the model. The value of $S_{g,max}$ is 0.8 and the value of $S_{gt,max}$ for the calculation of residual trapped gas saturation is 0.4. Figure 4 shows the total gas saturations at 2020-01-01 and at 2040-01-01 for the case without hysteresis in the relative permeability curves (i.e. k_{rg} follows the drainage curve in Figure 1) and the case with hysteresis (i.e. k_{rg} follows Land's model). As the CO_2 bubble rises, water flows downward. This counter-current flow induces imbibition and traps residual gas below the cap rock (Figures 4(b) and 4(d)). Without the hysteresis effects, most of the CO_2 is found to migrate to the top of the reservoir (Figure 4(c)).

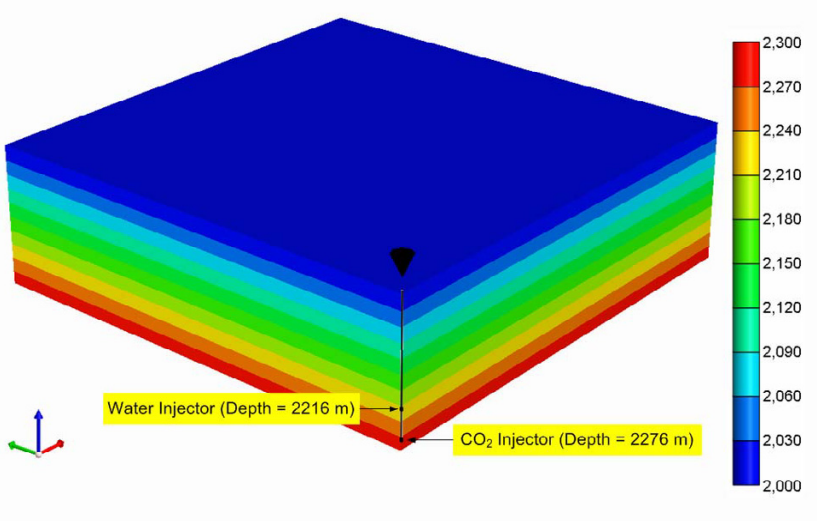

Figure 2: Aquifer Element of Symmetry
(The displayed value is the depth of the grid top in m)

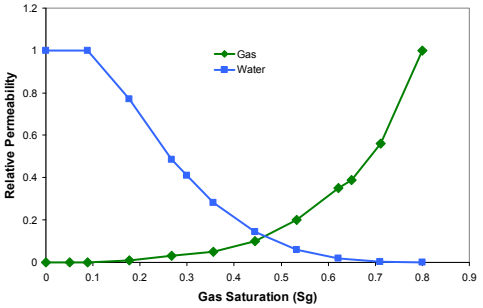

Figure 3: Relative Permeability Curves

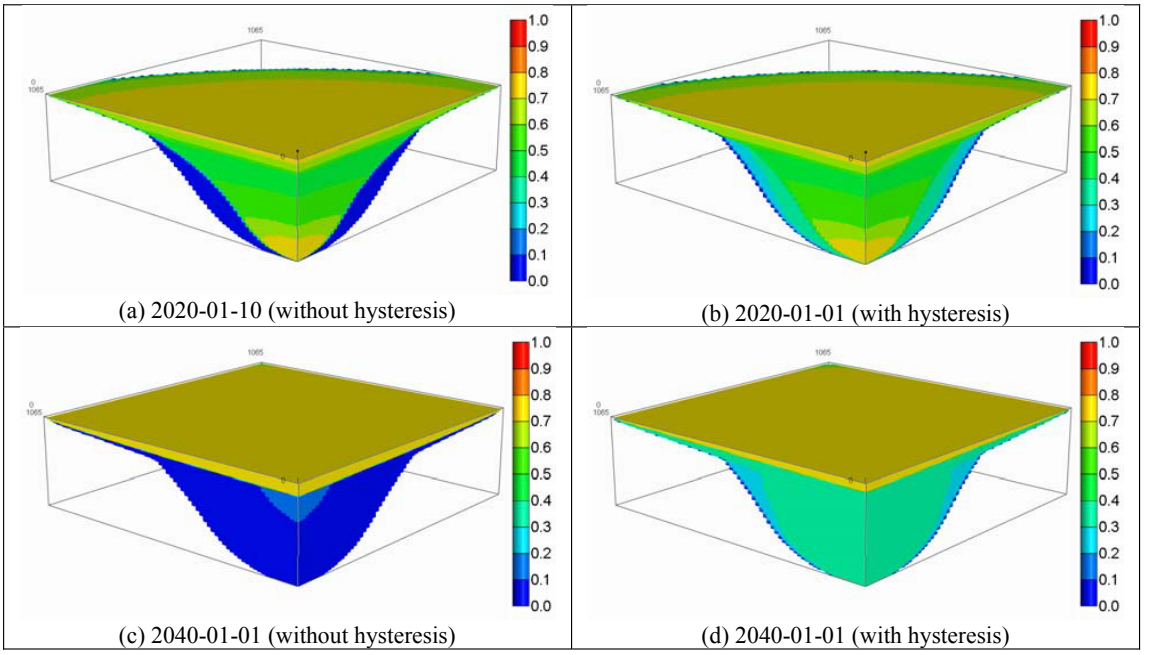

(a) 2020-01-10 (without hysteresis)

(b) 2020-01-01 (with hysteresis)

(c) 2040-01-01 (without hysteresis)

(d) 2040-01-01 (with hysteresis)

Figure 4 – Gas saturation after 20 years and 40 years (CO_2 was injected for 25 years)

3. Acceleration of Residual Gas Trapping through Water Injection

Residual gas trapping is caused by water imbibition. In the above example, this imbibition is induced by the natural downward flow of water with the rising CO_2 bubble. It is conceivable that the simultaneous injection of water during the CO_2 injection would promote additional imbibition and therefore would accelerate and increase the amount of residual gas trapping. Figure 2 shows the location of the water injector, which is completed at a depth of 2216 m (60 m above the CO_2 injector). In Run 2, brine with the same salinity is injected at a rate of 2960 reservoir m^3/day, which is about the same as the CO_2 volumetric injection rate at reservoir conditions. Figure 5 shows the residual gas saturation and the total gas saturation at 2020-01-01 and 2040-01-01. Brine injection into the upper well prevents the CO_2 bubble from rising and the CO_2 spreads further into the formation as illustrated in Figure 5(a). After brine injection is stopped, countercurrent flow of CO_2 and water traps a substantial amount of CO_2 as residual gas as depicted in Figure 5(d).

The above example shows that water injection can be used to accelerate and increase the amount of residual gas trapping. There is a competition between residual gas trapping and solubility trapping. As the amount of residual gas trapping increases, there is less dissolution of CO_2 in brine. This offers the opportunity to maximize the total trapped amount by optimizing the water injection process. In the following an optimization procedure was applied to determine the rate, duration and location that would maximize the total trapped amount. Qi et al. (2007) investigated the co-injection of CO_2 and brine at the same location followed by chase brine. The process discussed in this paper is different as brine is injected above CO_2 to (1) help spread the CO_2 bubble and (2) enhance residual gas trapping through counter current flow after the end of water injection.

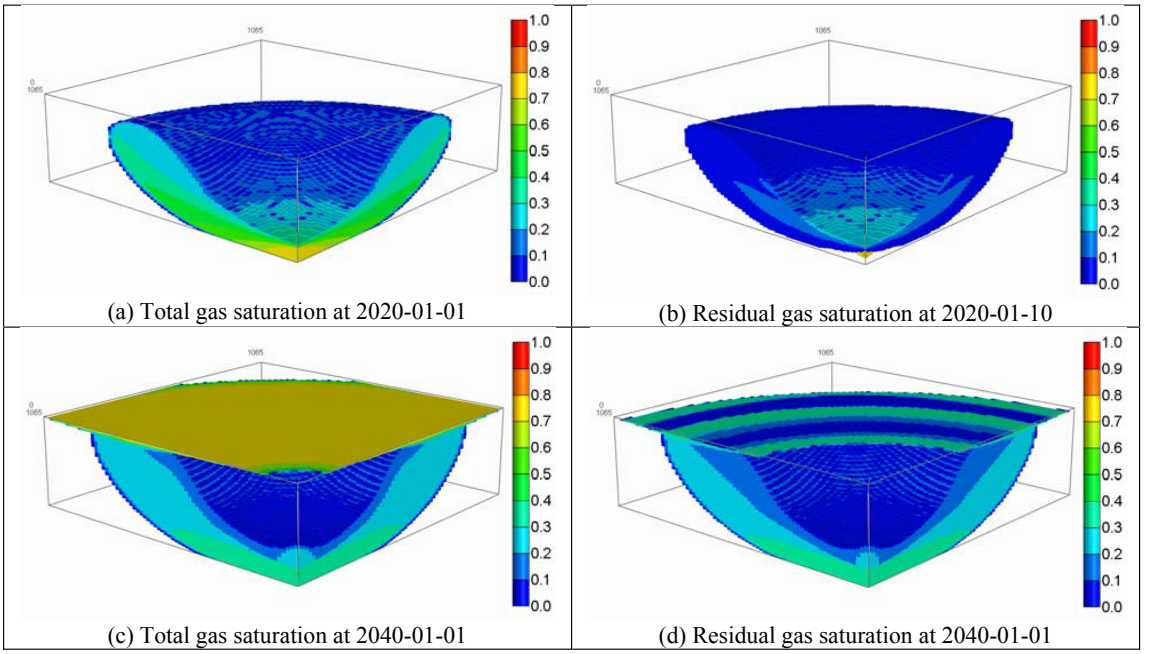

(a) Total gas saturation at 2020-01-01 (b) Residual gas saturation at 2020-01-10

(c) Total gas saturation at 2040-01-01 (d) Residual gas saturation at 2040-01-01

Figure 5 – Total gas saturation and trapped gas saturation after 20 years and 40 years (CO_2 and water were injected for 25 years)

4. Optimization of Trapped CO_2

The optimization parameters are shown in Table 1:

Table 1 – Operating parameters

Parameter	*Description*	*Values*
H2OBHW	Water rate at reservoir condition (m^3/day)	1480, 2960, 4440, 5920
H2OPERF	Depth of water injector (m)	2096, 2156, 2216
H2OPERIOD	Water injection period (years)	10, 15, 20, 25

The optimization is performed for two aquifers, one with low permeabilities (k_h = 100 md; k_v = 10 md) and one with high permeabilities (k_h = 500 md; k_v = 50 md). The optimization procedure is a combination of evolutionary methods combined with Tabu search. This optimization procedure was successfully applied in history matching and NPV optimization (Yang et al., 2007a, 2007b). In this paper, the following trapping indices are defined:

$$\text{Residual Gas Trapping Index RTI(t)} = \frac{\text{Total mass of } CO_2 \text{ trapped as residual gas at time t}}{\text{Total mass of } CO_2 \text{ injected at time t}} \tag{3a}$$

$$\text{Solubility Trapping Index STI(t)} = \frac{\text{Total mass of } CO_2 \text{ soluble in brine at time t}}{\text{Total mass of } CO_2 \text{ injected at time t}} \tag{3b}$$

$$\text{Trapping Efficiency Index TEI(t)} = \text{RTI(t)} + \text{STI(t)} \tag{3c}$$

Two objective functions are considered: J_1 = TEI (25 years) and J_2 = TEI (50 years). With J_1 and J_2, the total trapped amounts at 25 years and 50 years are maximized, respectively. The results of the optimization are summarized in Table 2.

For the low-permeability aquifer, the optimal operating conditions consist of injecting water at the maximum rate of 5920 res. m^3/day and at the largest depth (2216 m). For a maximum TEI at 25 years, the period of injection is 15 years giving rise to a value of TEI of 0.621 (RTI = 0.439; STI = 0.182). For a maximum TEI at 50 years, the period of injection is 20 years giving rise to a value of TEI of 0.971 (RTI = 0.742; STI = 0.230).

For the high-permeability aquifer, the operating conditions for a maximum value of TEI at 25 years consist of injecting water at the maximum rate of 5920 res. m^3/day, at the largest depth (2216 m) and for a period of 20 years. The corresponding TEI, RTI and STI are respectively 0.728, 0.217 and 0.511. The maximum value for TEI at 50 years correspond to injecting water at a rate of 2,960 res. m^3/dat, at a depth of 2156 m and for a period of 10 years. The corresponding TEI, RTI and STI are respectively 0.929, 0.237 and 0.693.

The above examples show that residual trapping is significant in low-permeability aquifers while solubility trapping is more dominant in high-permeability aquifers. The operating conditions that maximize the trapping at 25 years are not the same as those that maximize the trapping at 50 years. Note that the optimal conditions correspond to the parameter values listed in Table 1. There are conditions besides the values listed that would give a better RTI, STI and TEI.

Figure 6 shows the evolution of the amounts of residual gas trapping, solubility trapping and total trapping as functions of time for the optimal J_2 case in the low-permeability aquifer and high-permeability aquifer. Results for the cases without water injection are also shown. The following observations can be made:

- Residual gas trapping increases after the shut-in of the water injector as counter current flow is accelerated.
- For the high-permeability aquifer, a second step increase in residual gas trapping occurs after the shut-in of the CO_2 injector.
- Residual gas trapping prevails in low-permeability aquifers while solubility trapping dominates in high-permeability aquifers.
- For the high-permeability aquifer considered here, water injection does not increase total amount of trapped CO_2.
- For the low-permeability aquifer considered here, a substantial increase in the total amount of trapped CO_2 can be achieved with water injection (from 80.0% to 97.1%)
- The above examples show that the total trapping for the low-permeability aquifer is larger than the one for the high-permeability aquifer. However, this may not be always the case.

5. Conclusion

This paper discusses the two most important trapping mechanisms in CO_2 storage in saline aquifers, namely residual gas trapping and solubility trapping. It is shown that water injection can be used to enhance the amount of residual gas trapping as well as the amount of solubility trapping. Optimal location and operating conditions for the water injector are determined to maximize the total trapping of CO_2 for a low-permeability aquifer and a high-permeability aquifer. It is shown that low vertical permeability and water injection at a larger depth favor residual gas trapping while high vertical and horizontal permeability and water injection at a smaller depth favor solubility

trapping. It is also shown that water injection does not increase the total trapping for high permeability aquifers but improves substantially the total trapping in low-permeability aquifers. To simplify the analysis of residual gas trapping and solubility trapping, the aquifers considered in this paper have homogeneous properties. Heterogeneities will certainly affect the results. In particular, barriers to vertical flow will increase the amounts of residual gas trapping. In addition, economics calculations are not considered for the addition of a water injector in the CO_2 storage process.

Table 2 – Optimal Operating Conditions for CO_2 Trapping

k_h = 100 md; k_v = 10 md				
Wat. Inj. Rate (res. m^3/day)	Wat. Inj. Perf. (m)	Wat. Inj. Period (years)	J_1 TEI (25 years)	J_2 TEI (50 years)
5920	2216	15	0.621	0.932
5920	2216	20	0.607	0.971
k_h = 500 md; k_v = 50 md				
Wat. Inj. Rate (res. m^3/day)	Wat. Inj. Perf. (m)	Wat. Inj. Period (years)	J_1 TEI (25 years)	J_2 TEI (50 years)
5920	2216	20	0.728	0.911
2960	2156	10	0.682	0.929

References

Ennis-King, J. and Paterson, L.: "Engineering Aspects of Geological Sequestration of Carbon Dioxide," paper SPE 77809, *Proceedings* of the Asia Pacific Oil and Gas Conference and Exhibition, Melbourne, Australia, 8-10 October 2002.

Juanes, R., Spiteri, E.J., Orr, F.M. Jr. and Blunt, M.J.: "Impact of Relative Permeability Hysteresis on Geological CO_2 Storage," *Water Resources Research*, Vol. 42 (2006) W12418.

Kumar, A., Ozah, R., Noh, M., Pope, G.A., Bryant, S., Sepehrnoori, K. and Lake, L.: "Reservoir Simulation of CO_2 Storage in Deep Saline Aquifers," *SPEJ*, Vol. 10 (September 2005) 336-348.

Leonenko, Y., Keith, D.W., Pooladi-Darvish, M. and Hassanzadeh, H.: "Accelerating the Dissolution of CO_2 in Aquifers," *Proceedings* GHGT-8, 8-th International Conference on Greenhouse Gas Control Technologies, Trondheim, Norway, 19-22 June 2006.

Land, C.S.: "Calculation of Imbibition Relative Permeability for Two- and Three-Phase Flow from Rock Properties," *Soc. Pet. Eng. J.*, Vol. 8, No. 2 (June 1968) 149-156.

Nghiem, L., Sammon, P., Grabenstetter, J. and Ohkuma, H.: "Modeling CO_2 Storage in Aquifers with a Fully-Coupled Geochemical EOS Compositional Simulator," *Proceedings* 2004 SPE/DOE Fourteenth Symposium on Improved Oil Recovery Tulsa, Oklahoma, U.S.A., 17–21 April 2004.

Obi, E-O.J. and Blunt, M.J.: "Streamline-Based Simulation of Carbon Dioxide Storage in a North Sea Aquifer," *Water Resources Research*, Vol. 42 (2006) W03414.

Qi, R., Beraldo, V., LaForce, T. and Blunt, M.J.: "Design of Carbon Dioxide Storage in a North Sea Aquifer Using Streamline-Based Simulation," paper SPE 109905, *Proceedings* 2007 Annual Technical Conference and Exhibition, Anaheim, California, U.S.A., 11–14 November 2007.

Spiteri, E.J., Juanes, R., Blunt, M.J. and Orr, F.M. Jr.: "Relative Permeability Hysteresis: Trapping Models and Application to Geological CO_2 Sequestration," paper SPE 96448, *Proceedings* 2005 Annual Technical Conference and Exhibition, Dallas, Texas, U.S.A. 9-12 October 2005.

Taku Ide, S., Jessen, K. and Orr, F.M. Jr.: "Storage of CO_2 in Saline Aquifers: Effects of Gravity, Viscous, and Capillary Forces on Amount and Timing of Trapping," *International Journal of Greehouse Gas Control* (2007) 481-491.

Thibeau, S., Nghiem, L.X. and Ohkuma, H.: "A Modeling Study of Selected Minerals in Enhancing CO_2 Mineralization During CO_2 Aquifer Storage," paper SPE 109739, *Proceedings* 2007 SPE Annual Technical Conference and Exhibition, Anaheim, California, U.S.A., 11-14 November 2007.

Yang, C., Card, C.C. and Nghiem, L.: "Economic Optimization and Uncertainty Assessment of Commercial SAGD Operations," paper 2007-029, *Proceedings* Canadian International Petroleum Conference, June 11-14, 2007a, Calgary, Alberta, Canada.

Yang, C., Nghiem, L., Card, C. and Bremeier, M.: "Reservoir Model Uncertainty Quantification through Computer-Assisted History Matching," paper SPE 109825, presented at the 2007 SPE Annual Technical Conference and Exhibition, Anaheim, California, U.S.A., 11-14 November 2007b.

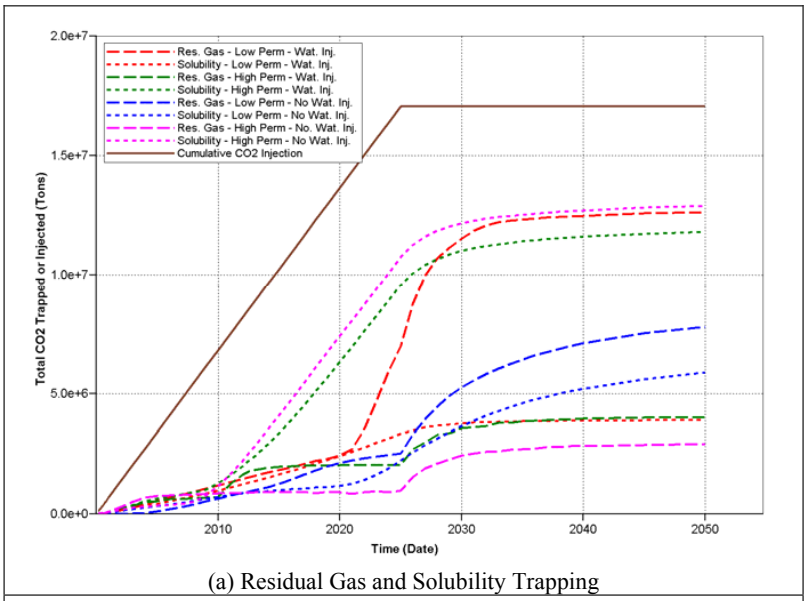

(a) Residual Gas and Solubility Trapping

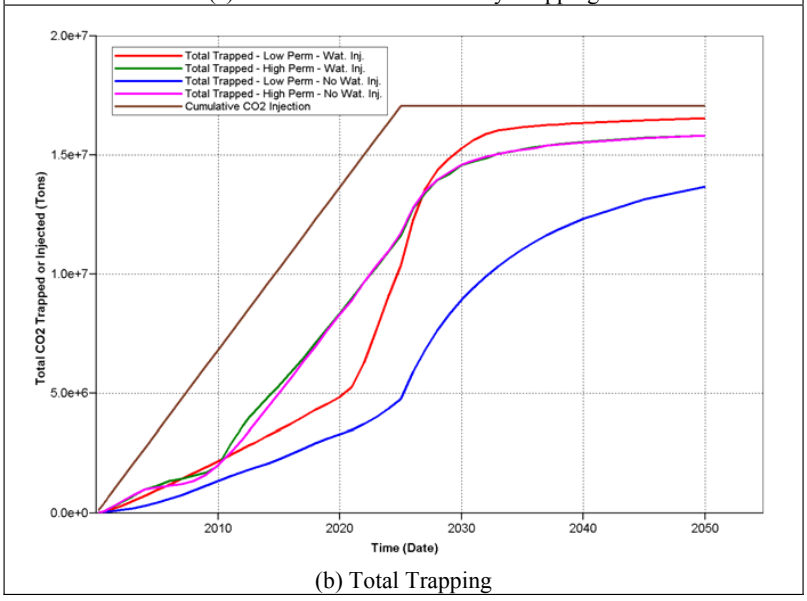

(b) Total Trapping

Figure 6: Evolution of Residual Gas Trapping, Solubility Trapping and Total Trapping